Stem Cell Research (2015) 14, 185–197

Available online at www.sciencedirect.com

ScienceDirect

www.elsevier.com/locate/scr

Cell aggregation optimizes the differentiation of human ESCs and iPSCs into pancreatic bud-like progenitor cells

Taro Toyoda[a], Shin-Ichi Mae[a], Hiromi Tanaka[a], Yasushi Kondo[a,b], Michinori Funato[a,c], Yoshiya Hosokawa[a,d], Tomomi Sudo[a], Yoshiya Kawaguchi[a], Kenji Osafune[a,*]

[a] *Center for iPS Cell Research and Application (CiRA), Kyoto University, 53 Kawahara-cho, Shogoin, Sakyo-ku, Kyoto 606-8507, Japan*
[b] *Department of Diabetes and Clinical Nutrition, Graduate School of Medicine, Kyoto University, 54 Kawahara-cho, Shogoin, Sakyo-ku, Kyoto 606-8507, Japan*
[c] *Department of Clinical Research, National Hospital Organization, Nagara Medical Center, 1300-7 Nagara, Gifu 502-0071, Japan*
[d] *Department of Metabolic Medicine, Osaka University Graduate School of Medicine, 2-2 Yamadaoka, Suita 565-0871, Japan*

Received 15 August 2014; received in revised form 28 December 2014; accepted 19 January 2015
Available online 28 January 2015

Abstract Embryonic pancreatic bud cells, the earliest pancreas-committed cells, generated from human embryonic stem cells (hESCs) and induced pluripotent stem cells (hiPSCs) have been shown to differentiate into mature pancreatic β-cells *in vivo*, indicating the feasibility of hESC/iPSC-based cell therapy for diabetes. However, the key factors required for the differentiation of these cells into pancreatic bud cells are incompletely understood. The purpose of this study was to establish culture conditions that efficiently induce PDX1$^+$NKX6.1$^+$ pancreatic bud cells from hESCs/iPSCs. We differentiated a hESC line, KhES-3, into pancreatic lineages with a stepwise protocol recapitulating developmental process. The induction rate of PDX1$^+$NKX6.1$^+$ cells was correlated with cell density in adherent cultures, and markedly improved with cell aggregation cultures. The positive effects of cell aggregation cultures on the differentiation of pancreatic bud cells were reproduced in multiple hESC/iPSC lines. The human PDX1$^+$NKX6.1$^+$ cells developed into pancreatic epithelia after implantation into immunocompromised mice. Moreover, human C-peptide secretion into mouse bloodstream was stimulated by glucose challenges after *in vivo* maturation. Taken together, these results suggest that cultures with high cell density are crucial for the differentiation of pancreas-committed progenitor cells from hESCs/iPSCs. Our findings may be applicable for the development of hESC/iPSC-based cell therapy for diabetes.

Introduction

Diabetes is caused by an absolute or relative insufficiency of insulin which is secreted from pancreatic β-cells, resulting in impaired glucose metabolism in the entire body (Mathis and

* Corresponding author. Fax: +81 75 366 7077.
E-mail address: osafu@cira.kyoto-u.ac.jp (K. Osafune).

http://dx.doi.org/10.1016/j.scr.2015.01.007
1873-5061/

Vence, 2001; Donath and Halban, 2004). The supplementation of β-cell function is an effective therapeutic strategy, but the insufficient cell supply is a major obstacle to this intervention (Matsumoto, 2011). Therefore, vigorous efforts have been made to develop a stable source of pancreatic cells for clinical use.

Human embryonic stem cells (hESCs) and induced pluripotent stem cells (hiPSCs) are attractive cell sources due to their potential for unlimited proliferation and differentiation (Dominguez-Bendala et al., 2011; McCall et al., 2010). Indeed, a number of groups have generated immature pancreatic β cell-like cells, which are referred to as insulin-producing or insulin-secreting cells, from hESCs/iPSCs *in vitro* (D'Amour et al., 2006; Jiang et al., 2007a,b; Zhang et al., 2009; Nostro et al., 2011; Kroon et al., 2008; Mfopou et al., 2010; Shim et al., 2007; Cai et al., 2010; Kelly et al., 2011; Xu et al., 2011; Kunisada et al., 2012; Rezania et al., 2011, 2012, 2013; Schulz et al., 2012; Bruin et al., 2013; Sui et al., 2013). Despite the difficulties in generating genuine β-cells *in vitro*, mature insulin-producing cells with the potential for glucose responsiveness have been obtained following the implantation of hESC-derived pancreatic progenitors into immunodeficient mice (D'Amour et al., 2006; Kroon et al., 2008; Shim et al., 2007; Kelly et al., 2011; Rezania et al., 2012, 2013; Bruin et al., 2013). Therefore, implantation of pancreatic progenitors, instead of β-cells, is also considered to be a therapeutic option for diabetes.

Previous reports have described the generation of pancreatic lineage cells, such as pancreatic progenitors and insulin-producing cells, from hESCs/iPSCs *in vitro*, using stepwise differentiation protocols that recapitulate pancreatic development (D'Amour et al., 2006; Jiang et al., 2007a, b; Zhang et al., 2009; Nostro et al., 2011; Kroon et al., 2008; Mfopou et al., 2010; Shim et al., 2007; Cai et al., 2010; Kelly et al., 2011; Xu et al., 2011; Kunisada et al., 2012; Rezania et al., 2011, 2012, 2013; Schulz et al., 2012; Bruin et al., 2013; Sui et al., 2013). However, the quantitative differences in the differentiation efficiency among hESC/iPSC lines make it difficult to obtain the stable production of pancreatic lineage cells with sufficient purity for use in the clinical setting (Osafune et al., 2008). One of the solutions for this is the establishment of stable differentiation methods that can be more broadly applied to multiple hESC/iPSC lines, based on a complete understanding of the mechanisms of pancreatic organogenesis.

The major components of the pancreas are exocrine, duct and endocrine cells, which originate from the endoderm layer of early embryos marked by the co-expression of transcription factors Sox17 and FoxA2 (Jennings et al., 2013). The endodermal layer extends and folds to form the primitive gut tube expressing Hnf1β and Hnf4α, which has potential to differentiate into respiratory apparatus, digestive tract and endocrine organs, including the pancreas. Distinct pancreatic organogenesis morphologically starts at the posterior foregut area in the primitive gut tube following the expression of a transcription factor, Pdx1 (Jorgensen et al., 2007; Jensen, 2004). Two parts of the Pdx1$^+$ gut tube thicken to form the dorsal and ventral pancreatic buds. It should be noted that the early pancreatic epithelia formed by the stratification of the single cell layer of the gut tube and its protrusion into the surrounding mesenchyme exist as a three-dimensional highly-dense aggregate expressing additional transcription factors, Ptf1a and Nkx6.1, during the process of bud formation (Hald et al., 2008; Ahnfelt-Ronne et al., 2012; Kawaguchi et al., 2002; Villasenor et al., 2010). After that, microlumens appear and fuse to form epithelial structures with a branched tubular network within the aggregated pancreatic buds. Some epithelia differentiate into hormone-producing endocrine lineages, such as insulin-secreting β-cells and glucagon-secreting α-cells, and migrate into the mesenchyme to form pancreatic islets. Therefore, during the long process of islet formation, cells experience dynamic structural changes.

The Pdx1 expression is first detected at the presumptive bud area, maintained throughout the entire pancreatic development and eventually localized to β- and δ-cells (Jorgensen et al., 2007; Serup et al., 1995). However, the Pdx1 expression is not exclusive to the pancreas in gut tube, and extends anteriorly into the posterior stomach, duodenum and biliary system in the middle of embryogenesis (Jorgensen et al., 2007; Fukuda et al., 2006). On the other hand, the expression of Nkx6.1 and Ptf1a is found only in Pdx1$^+$ pancreatic buds and these are specific for pancreatic epithelium. Nkx6.1 and Ptf1a expression is eventually restricted to β- and exocrine acinar cells, respectively (Hald et al., 2008; Oster et al., 1998; Pan et al., 2013). Therefore, pancreatic bud cells co-expressing Pdx1, Ptf1a and Nkx6.1 are considered to be the earliest pancreas-committed progenitors. In fact, the results of implantation experiments have demonstrated that the PDX1$^+$NKX6.1$^+$ cells are progenitors that specifically differentiate into pancreatic cells (Kelly et al., 2011; Rezania et al., 2013).

In the current study, we evaluated the morphological characteristics of the pancreatic bud formation and tested the hypothesis that a high cell density is a key factor required to induce pancreatic bud cells in hESC/iPSC cultures. For this purpose, we compared the induction efficiency of the PDX1$^+$NKX6.1$^+$ cells in aggregation cultures with that in planar culture conditions, and performed the implantation of the PDX1$^+$NKX6.1$^+$ cells into immunocompromised mice to confirm whether the generated cells had the potential to differentiate into pancreatic lineages *in vivo*. We found that a high cell density is a crucial factor to induce PDX1$^+$NKX6.1$^+$ pancreatic bud cells *in vitro*, which can further differentiate into pancreatic epithelia and mature into functional endocrine cells *in vivo*. We also found that NKX6.1$^+$ cells originated from PDX1^{high} cells among heterogeneous PDX1$^+$ cell populations.

Material and methods

In vitro differentiation of hESCs/iPSCs

The maintenance culture of a hESC line, KhES-3 (Suemori et al., 2006), and five hiPSC lines; 585A1, 604B1, 692D2, 648B1 and 409B2 (Okita et al., 2011; Kajiwara et al., 2012) was performed as described previously (Mae et al., 2013). For feeder-free cultures, cells were maintained with Essential 8 medium (Thermo Fisher Scientific, Waltham, MA) according to the manufacturer's instructions. Experiments with hESCs/

iPSCs were approved by the ethics committee of the Department of Medicine and Graduate School of Medicine, Kyoto University. Cells were directed into key stages of pancreatic development, including definitive endoderm (Stage 1), primitive gut tube (Stage 2), posterior foregut (Stage 3) and pancreatic bud (Stage 4). The final protocol was as follows (Fig. 1A):

Stage 1 hESC/iPSC colonies grown on a feeder layer were first deprived of feeder cells and dissociated into

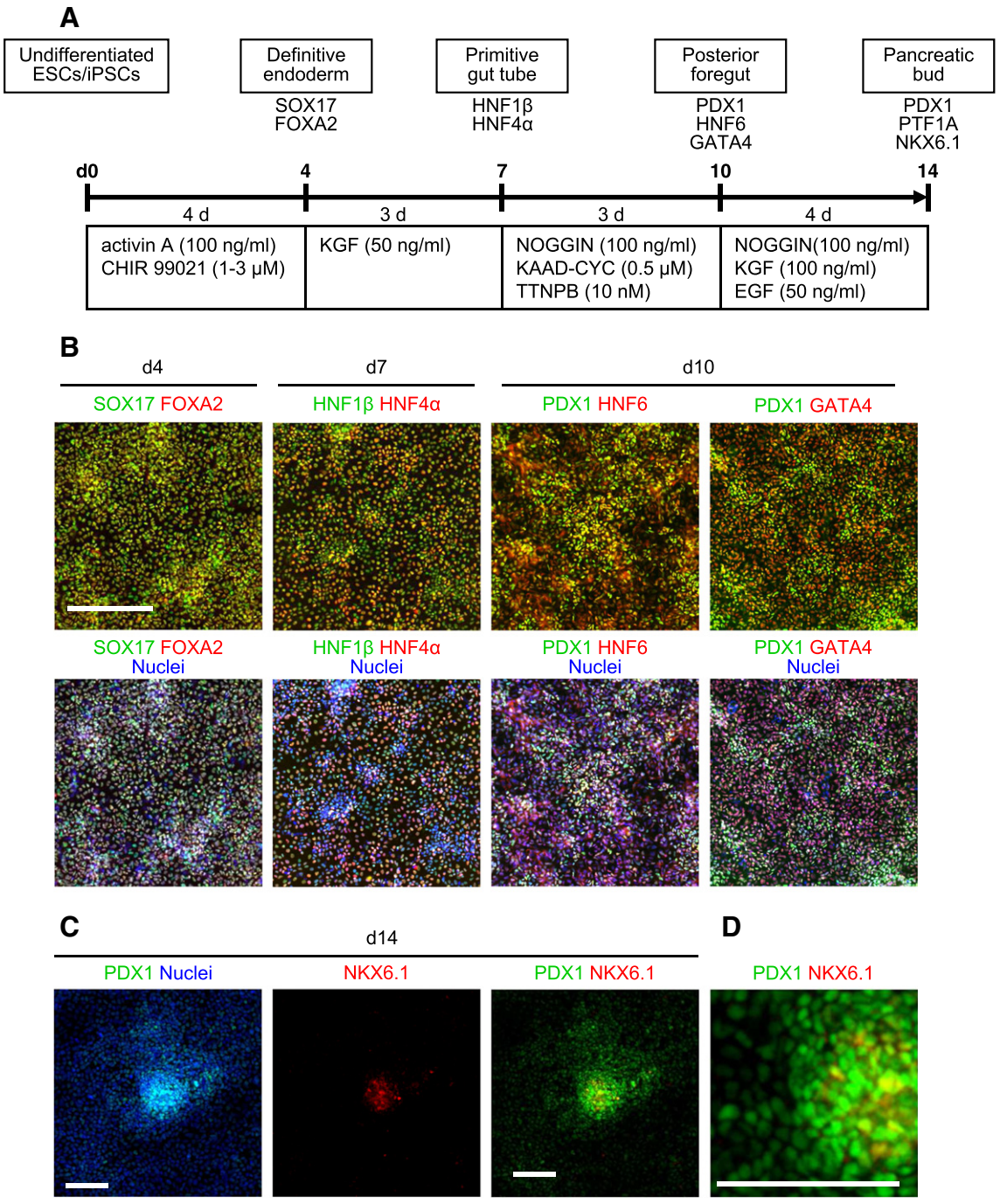

Figure 1 PDX1^{+}NKX6.1^{+} cells are localized at aggregated areas. (A) A schematic diagram of the procedures used for the differentiation of pancreatic bud cells from human ESCs. (B–D) A hESC line, KhES-3, was differentiated into definitive endoderm, primitive gut tube endoderm, posterior foregut and pancreatic bud, and was analyzed by immunostaining for representative markers. (D) A magnified image of (C). Note that only the aggregated areas of PDX1^{high} cells co-expressed NKX6.1. SOX17, SRY (sex determining region Y)-box17; FOXA2, forkhead box protein A2; HNF, hepatocyte nuclear factor; PDX1, pancreatic and duodenal homeobox 1; GATA4, GATA binding protein 4; NKX6.1, NK6 transcription factor related, locus 1. Scale bars, 300 μm in B and 100 μm in C and D.

single cells as described previously (Suemori et al., 2006). The cells were resuspended with Stage 1 medium containing RPMI 1640 medium (NACALAI TESQUE, Kyoto, Japan) supplemented with 2% (vol/vol) growth factor reduced B27 (GFR-B27, Thermo Fisher Scientific), 50 U/ml penicillin/streptomycin (P/S, Thermo Fisher Scientific), 100 ng/ml activin A (R&D Systems, Minneapolis, MN), 3 μM CHIR99021 (Axon Medchem, Groningen, Netherlands) and 10 μM Y-27632 (Wako, Osaka, Japan), seeded on Matrigel (Becton Dickinson, Franklin Lakes, NJ)-coated plates at a density of 1×10^5 cells/cm^2 and cultured for one day. For the next three days, the cells were cultured in RPMI 1640 medium with 2% GFR-B27, 50 U/ml P/S, 100 ng/ml activin A and 1 μM CHIR99021.

Stage 2 The cells were exposed to Improved MEM Zinc Option (iMEM) medium (Thermo Fisher Scientific) supplemented with 1% GFR-B27, 100 U/ml P/S (iMEM-B27) and 50 ng/ml keratinocyte growth factor (KGF; R&D Systems) for three days.

Stage 3 The cultures were continued for three days in iMEM-B27 with 0.5 μM 3-Keto-N-aminoethyl-N′-aminocaproyldihydrocinnamoyl cyclopamine (KAAD-CYC; Toronto Research Chemicals, Ontario, Canada), 0.5 nM 4-[(E)-2-(5,6,7,8-Tetrahydro-5,5,8,8-tetramethyl-2-naphthalenyl)-1-propenyl] benzoic acid (TTNPB, Santa Cruz Biotechnology, Dallas, TX) and 100 ng/ml NOGGIN (Pepro-tech, Rocky Hill, NJ).

Stage 4 The cells were cultured for four to 20 days in iMEM-B27 with 100 ng/ml KGF, 100 ng/ml NOGGIN and 50 ng/ml epidermal growth factor (EGF, R&D Systems). For monolayer and aggregation cultures, the cells after Stage 3 treatments were dissociated into single cells by gentle pipetting after treatment with 0.25% trypsin–EDTA. The same inducing factors were used as described above, except for the addition of 10 μM Y-27632 to the Stage 4 treatments. For monolayer cultures, the cells were seeded on Matrigel-coated plates at a density of 6–48×10^4 cells/cm^2. To evaluate various extracellular matrices, the cells were seeded on laminin-111 (10 μg/ml; BioLamina, Sundbyberg, Sweden), fibronectin (5 μg/ml, Merck, Whitehouse Station, NJ), Synthemax (Corning, Corning, NY) and collagen I plates (Becton Dickinson). For aggregation cultures, the cells were seeded on a low-binding plate at a density of $3–30 \times 10^3$ cells/well.

Immunostaining

The cells were fixed with 4% paraformaldehyde (PFA) for 20 min at 4 °C. Then, immunostaining was performed as described previously (Mae et al., 2013). The primary antibodies used are detailed in Supplementary Table 1. The cell aggregates or implanted grafts were fixed with 4% PFA for one to two days at 4 °C. After washing with PBS, the samples were equilibrated in a 10–30% sucrose solution at room temperature for 1 h, and then mounted and frozen. The frozen blocks were sectioned at 10–30 μm, and immunostaining was performed after removing the mounting medium. For quantification of the Ki-67$^+$ and cleaved-Caspase3$^+$ cell ratios, immunostained cells were analyzed using an image analyzer CellInsight NXT (Thermo Fisher Scientific, Waltham, MA) or manual counting.

Flow cytometry

The cells were dissociated into single cells with 0.25% trypsin–EDTA treatment, fixed, permeabilized and blocked with a BD Cytofix/Cytoperm Kit (Becton Dickinson). Then, cells were stained with the antibodies detailed in Supplementary Table 1.

Quantitative real-time reverse transcription-polymerase chain reaction (qRT-PCR)

Total RNA was isolated from the cells with an RNeasy kit (Qiagen, Venlo, Netherlands), and cDNA was prepared with a ReverTra Ace qPCR RT Master Mix (TOYOBO, Osaka, Japan) and oligo (dT)20 primer, according to the manufacturer's instructions. The qRT-PCR analysis was carried out with SYBR Premix Ex Taq II (Takara, Otsu, Japan). The expression of each gene was normalized to the level of glyceraldehyde-3-phosphate dehydrogenase (GAPDH) expression. The primer sequences used are shown in Supplementary Table 2.

Animal studies and transplantation experiments

All animal experiments were performed in accordance with the Guidelines for Animal Experiments of Kyoto University. Male seven- to 14-week-old NOD.CB17-Prkdc^{scid}/J mice (NOD–SCID, Charles River Laboratories Japan, Yokohama, Japan) were maintained on a 12-h light/dark cycle with *ad libitum* access to a standard irradiated diet. Mice were anesthetized with inhalable isoflurane and received implants of hESC-derived cell aggregates after Stage 4. Stage 4 day 4 cell aggregates (30×10^3 cells/aggregate) were cultured in Stage 4 medium with or without an ALK5 inhibitor (Santa Cruz) for one to two additional days before implantation. Then, two hundred cell aggregates per mouse were implanted under a kidney subcapsule. At 30–210 days after implantation, the mice were sacrificed and the serial sections of grafts were examined by immunostaining, as described above.

The graft function was assessed by measuring human C-peptide levels in mouse plasma in response to glucose administration. The mice were fasted for >5 h, and a 30% glucose solution was administered by intraperitoneal injection at a dose of 3.0 g/kg body weight. Blood samples were collected prior to and at 30 min after the glucose administration *via* a tail vein into heparinized capillaries. The plasma human C-peptide level was analyzed by an ELISA (Mercodia, Uppsala, Sweden), according to the manufacturer's instructions. All metabolic analyses were performed in conscious and restrained animals.

Statistical analysis

The statistical analyses were performed using paired t-tests (SigmaStat 3.5, Systat, San Jose, CA). The differences between groups were considered significant for values of $p < 0.05$.

Results

hESC-derived PDX1$^+$NKX6.1$^+$ cells are formed at aggregated areas of adhesion cultures

To examine the differentiation of PDX1$^+$NKX6.1$^+$ pancreatic bud-like cells from a hESC line, KhES-3, we developed a directed differentiation protocol with a monolayer culture format by modifying the previously reported methods (Kunisada et al., 2012; Schulz et al., 2012) (Fig. 1A). As analyzed by immunostaining for representative markers for each step, we effectively obtained cells of the definitive endoderm (SOX17$^+$FOXA2$^+$), gut tube endoderm (HNF4α^+HNF1β^+) and posterior foregut (PDX1$^+$HNF6$^+$ or PDX1$^+$GATA4$^+$) (Fig. 1B).

Further differentiation of hESC-derived posterior foregut toward the pancreatic bud yielded only a small number of PDX1$^+$NKX6.1$^+$ cells. Most NKX6.1$^+$ cells were located in the aggregated areas composed of cells showing bright PDX1 fluorescent signals, whereas the PDX1$^+$NKX6.1$^-$ cells were mostly found in the remaining monolayered areas (Figs. 1C and D). The areas of PDX1$^+$NKX6.1$^+$ cells were expanded gradually around the aggregates (data not shown), thus indicating their further differentiation into PDX1$^+$NKX6.1$^+$ cells or the proliferation of PDX1$^+$NKX6.1$^+$ cells within the aggregates. Our observation of PDX1$^+$NKX6.1$^+$ cells in the aggregated areas of adhesion cultures was reminiscent of the pancreatic budding in mouse embryos (Jorgensen et al., 2007).

Aggregation cultures efficiently differentiate hESC-derived PDX1$^+$ foregut into PDX1$^+$NKX6.1$^+$ pancreatic buds

Next, to investigate whether cell aggregation itself is a factor to promote NKX6.1$^+$ cell differentiation, the PDX1$^+$ cells on culture day 10 were either treated with Stage 4 factors (S4F), or were dissociated and treated with Stage 4 factors in monolayer cultures at different cell densities (6–48 × 10^4 cells/cm^2) (S4F-2D) or in suspension cultures with cellular aggregates of different sizes (3–30 × 10^3 cells/aggregate) (S4F-AG) (Fig. 2A). On day 14, the S4F cells showed a mixture of aggregated and monolayered areas, while the cells treated with the S4F-2D formed monolayers without any aggregated areas (Fig. 2B). Before the induction on day 10, there were no PDX1$^+$NKX6.1$^+$ cells (Fig. 2C). The S4F cultures generated PDX1$^+$NKX6.1$^+$ cells at an 18 ± 5% induction rate. On the other hand, the induction rate of PDX1$^+$NKX6.1$^+$ cells was consistently lower (3–17%) in the S4F-2D cultures in a coating with various extracellular matrices (Fig. S1), and there was a tendency for the rate to increase as the cell density increased. Notably, the much higher induction rate of PDX1$^+$NKX6.1$^+$ cells (38–40%) was consistently obtained with the S4F-AG cultures, regardless of the size, compared with the S4F-2D cultures.

To validate the mRNA expression of pancreatic bud markers in the S4F-AG cultures (hereafter described as aggregation cultures), we performed qRT-PCR analyses at each time point during Stage 4. The *PDX1* expression was increased in aggregation cultures shortly after the start of Stage 4, while the expression level was not changed in the S4F-2D cultures (hereafter described as monolayer cultures) (Fig. 2D). The expression of pancreatic bud-specific markers, *PTF1A* and *NKX6.1*, also began to increase one day after the start of Stage 4, and progressively increased in aggregation cultures, while the expression in monolayer cultures remained extremely low.

The positive effects of aggregation cultures on the differentiation of pancreatic bud cells were reproduced in multiple hiPSC lines (585A1, 604B1, 648B1, 692D2 and 409B2), in addition to a hESC line, KhES-3 (Fig. 2E). These results suggest that high cell density cultures with cellular aggregation promoted the differentiation of multiple hESC/iPSC cell lines into pancreatic bud cells.

PDX1$^+$NKX6.1$^+$ cells emerge from PDX1^{high} cells in cellular aggregates

In our adhesion culture, we found that there was heterogeneity of the PDX1$^+$ cells in terms of the expression levels (Fig. 1D). We therefore performed flow cytometric analyses of the cell populations in cellular aggregates after 0–20 days of Stage 4 treatments to determine the origin of the NKX6.1$^+$ cells. Before the Stage 4 treatments, around 80% of the cells were PDX1$^+$, and the majority was PDX1^{middle} or PDX1^{low}. However, within one day after the Stage 4 treatments, the majority of the cells became PDX1^{high}. On day 2, the PDX1^{high} cells started to diverge into two populations: one population expressing NKX6.1 and the other showing downregulation of the PDX1 expression (Fig. 3A). The ratio of PDX1$^+$NKX6.1$^+$ cells was significantly increased during the first four to eight days of Stage 4, and reached around 90% on days 12–20 (Fig. 3B). The PDX1$^+$NKX6.1$^+$ cell ratio was similar regardless of the aggregate size (Fig. S2). These results imply that the lineage commitment to PDX1$^+$NKX6.1$^+$ cells occurs between days 2 and 8.

Next, we investigated the localization of PDX1$^+$NKX6.1$^+$ cells in the cellular aggregates. Immunostaining on cryosections of aggregates on days 4 and 12 of Stage 4 revealed that PDX1$^+$NKX6.1$^+$ cells were uniformly distributed inside aggregates (Figs. 4A and B). Notably, most PDX1^{high} cells were PDX1$^+$NKX6.1$^+$ and were co-stained for GATA4 and SOX9, other markers for the pancreatic bud (Jennings et al., 2013). As occurs during *in vivo* pancreatic development, the PDX1$^+$NKX6.1$^+$ cell areas were stratified to become thickened by day 12 (Fig. 4B), suggesting that the increase in the PDX1$^+$NKX6.1$^+$ cell ratio on days 4–20 might be mainly due to the proliferation of these cells. In fact, the total cell numbers were increased by 2-fold on culture day 12 in Stage 4 compared with that observed on days 1–4 (Fig. S3). Insulin$^+$ (INS$^+$) cells were one component of the PDX1$^+$NKX6.1$^-$ cells. These INS$^+$ cells were PDX1^{low}, and some of them were glucagon$^+$ (GCG$^+$). There were some INS$^-$ GCG$^+$ cells, some ghrelin$^+$ (GHR$^+$) cells and some somatostatin$^+$ (SST$^+$) cells, suggesting the lineage commitment into immature fetal endocrine cells (Rezania et al., 2012).

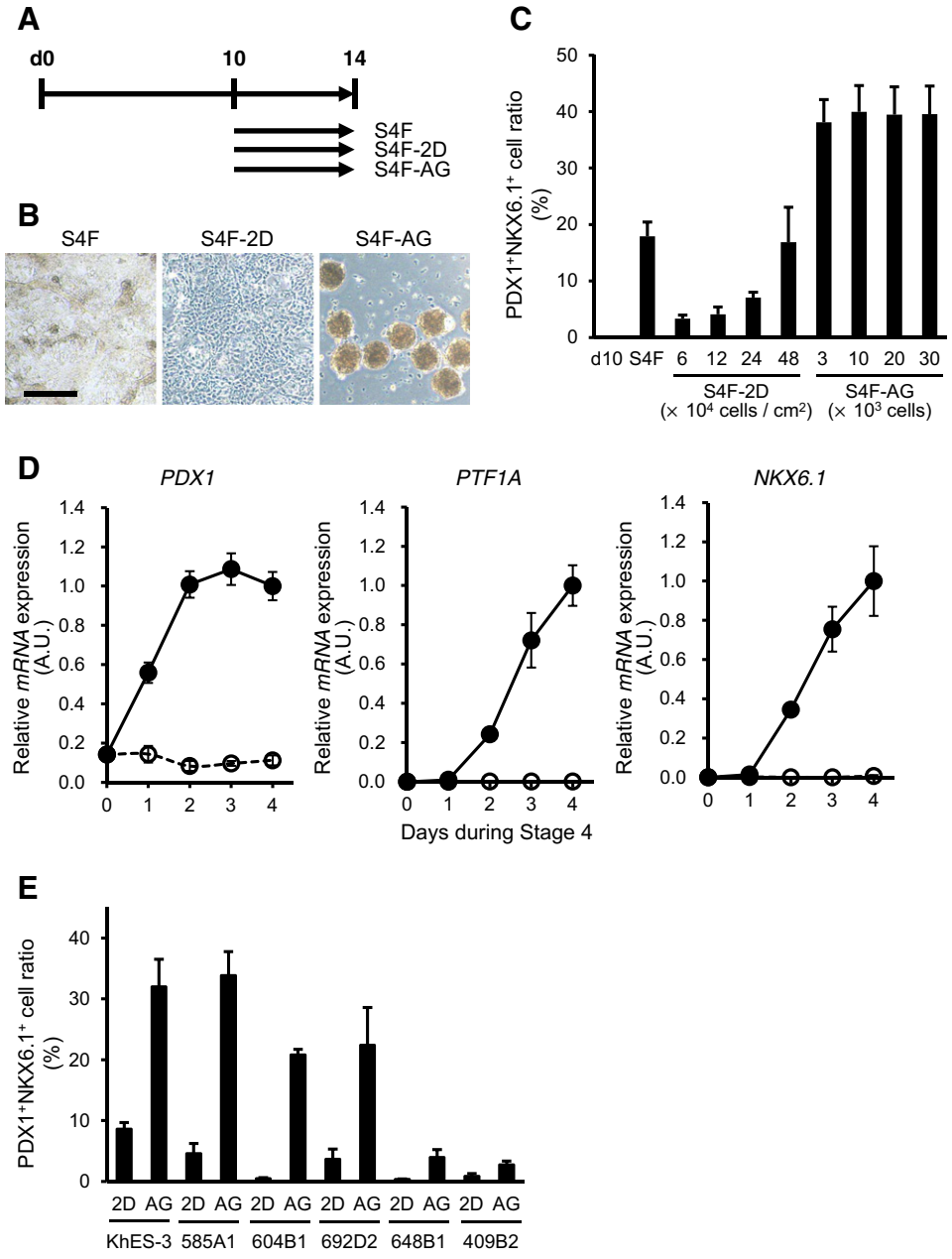

Figure 2 Cell aggregation cultures promote PDX1$^+$NKX6.1$^+$ cell induction from PDX1$^+$ posterior foregut cells. (A) A schematic diagram of the procedures used to assess the effects of the cell density on the cultures with regard to the induction of pancreatic bud cells. Posterior foregut cells differentiated in adhesion cultures were treated with the soluble factors required for pancreatic bud induction (KGF, NOGGIN and EGF), either with only a medium change (S4F) or with re-seeding at different cell densities for monolayer cultures (6–48 × 10^4 cells/cm^2, S4F-2D) or to form cellular aggregates (3–30 × 10^3 cells/aggregate) (S4F-AG). (B) Representative bright field images of the three culture formats. (C) Quantification of the PDX1$^+$NKX6.1$^+$ cell ratio. After the induction of pancreatic bud cells in the three culture conditions described above, cells were examined by flow cytometry. (D) The mRNA expression of pancreatic bud markers, *PDX1*, *PTF1A* and *NKX6.1*, was assessed by quantitative real-time polymerase chain reaction (qRT-PCR) before and during pancreatic bud induction with cell aggregation (black circle, solid line) and in monolayer cultures (open circle, dotted line). The data are presented as the fold-change in gene expression relative to the peak value. (E) A hESC line (KhES-3) and five hiPSC lines (585A1, 604B1, 692D2, 648B1 and 409B2) were differentiated into posterior foregut cells in adhesion cultures. Then, the foregut cells were dissociated, re-seeded either for monolayer cultures (12 × 10^4 cells/cm^2, 2D) or to form cellular aggregates (3 × 10^3 cells/aggregate, AG) and were treated with KGF, NOGGIN and EGF to induce pancreatic bud cells. After the differentiation, the PDX1$^+$NKX6.1$^+$ cell ratio was measured by flow cytometry. The data are presented as the mean ± S.E.M. from three to seven independent experiments in C and from three independent experiments in D and E. Scale bar, 300 μm.

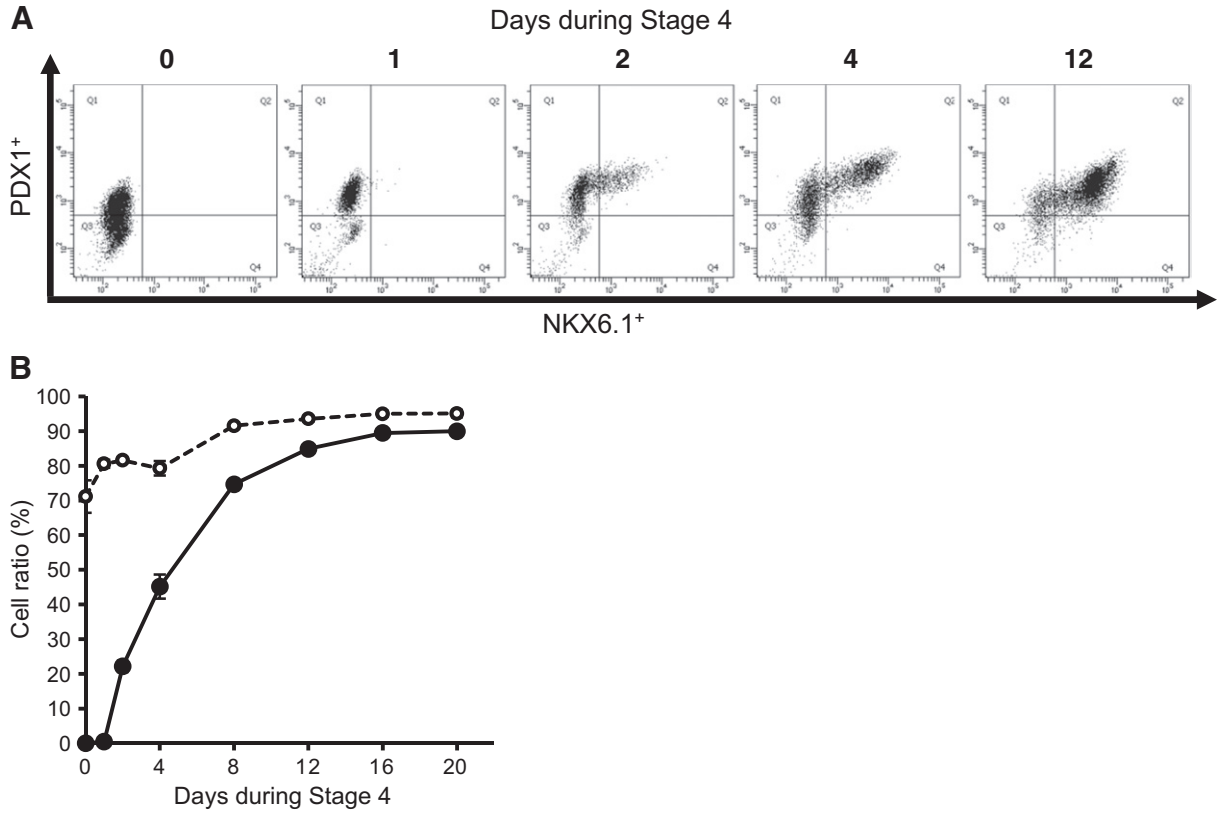

Figure 3 PDX1$^+$NKX6.1$^+$ cells emerge from PDX1^{high} cells in cellular aggregates. Cell populations were analyzed by flow cytometry after 0–20 days of aggregation culture at Stage 4. (A) Representative dot plots indicating that NKX6.1$^+$ cells emerged from PDX1^{high} cells. (B) Quantification of the induction rate of PDX1$^+$NKX6.1$^+$ (black circle, solid line) and the total PDX1$^+$ cells (open circle, dotted line). The data are from three independent experiments presented as the mean ± S.E.M.

The commitment to PDX1$^+$NKX6.1$^+$ cells requires both cell aggregation and soluble factors

A novel protocol combining the treatment with three soluble factors (KGF, NOGGIN and EGF) and cell aggregation cultures was established to efficiently induce the PDX1$^+$NKX6.1$^+$ cells in this study. Three soluble factors were also effective in inducing the *NKX6.1* gene expression in the adhesion cultures (S4F) (Schulz et al., 2012) (Fig. S4). To investigate whether the signals elicited by aggregation cultures were independent of those induced by the three factors, we examined the effects of all combinations of the factors on the *NKX6.1* expression after four-day treatments with aggregation cultures. The cellular aggregates did not express *NKX6.1* without any factor treatments, while the expression was increased by the treatments with each single factor or each combination of two factors out of the three, and the expression was highest when the cells were treated with all three factors (Fig. 5A). These data suggest that the signals elicited by aggregation cultures are independent of those induced by the three factors.

To determine the timing of the soluble factor treatments required for PDX1$^+$NKX6.1$^+$ cell commitment, cellular aggregates were cultured for 12 days, and NOGGIN or all three factors were removed for either the last four or eight days. The removal of NOGGIN did not significantly change the PDX1$^+$NKX6.1$^+$ cell ratio on day 12 (Fig. 5B). On the other hand, the removal of all three factors for the last four or eight days slightly decreased the PDX1$^+$NKX6.1$^+$ cell ratio on day 12, but the ratio was still increased compared to that before the removal. These results suggest that the cell fate commitment into PDX1$^+$NKX6.1$^+$ cells induced by soluble factors occurred by day 4 of Stage 4.

In order to examine whether the selection for PDX1$^+$NKX6.1$^+$ cell progenitors leads to an increase in the ratio of PDX1$^+$NKX6.1$^+$ cells in aggregation cultures, we performed time course analyses of the proliferating and apoptotic cells at Stage 4. The levels of proliferative cells were increased and few cells were apoptotic in the S4F and S4F-2D cultures (Fig. S5). The apoptotic cell ratio tended to be higher in the S4F-AG culture in the early periods of Stage 4 compared with that observed in the S4F and S4F-2D cultures. The apoptotic cell ratio decreased, while the proliferating cell ratio increased, with time in the S4F-AG culture. More apoptotic cells were found among the PDX1$^-$ cells than the PDX1$^+$ cells in the S4F-AG cultures, suggesting that the selection of PDX1$^+$ cells may be a mechanism underlying the increased rate of induction of PDX1$^+$NKX6.1$^+$ cells (Fig. S5D).

PDX1$^+$NKX6.1$^+$ cells differentiate into pancreatic epithelia *in vivo*

We next examined the developmental potential of the PDX1$^+$NKX6.1$^+$ cells generated with aggregation cultures to

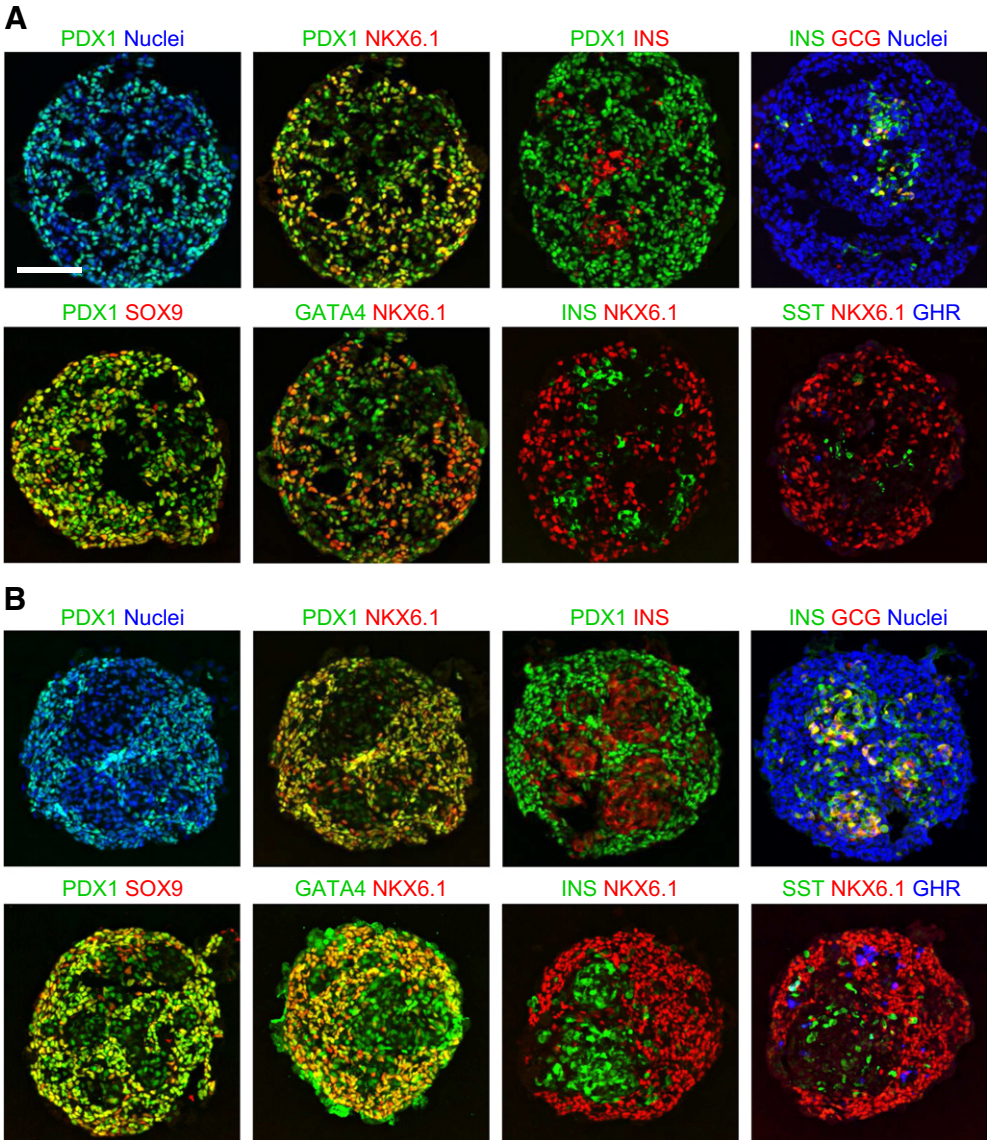

Figure 4 PDX1$^+$NKX6.1$^+$ cells in cellular aggregates co-express multiple pancreatic bud markers. The localization of PDX1$^+$NKX6.1$^+$ cells in aggregates was assessed. Cryosections of cellular aggregates at Stage 4, days 4 (A) and 12 (B), were stained for the indicated markers of pancreatic buds (PDX1, NKX6.1, SOX9 and GATA4) and endocrine cells (INS, GCG, SST and GHR). Pancreatic bud cells were distributed throughout the entire aggregates, and were segregated from endocrine compartments. SOX9, SRY (sex determining region Y)-box9; INS, insulin; GCG, glucagon; SST, somatostatin; GHR, ghrelin. Scale bar, 100 μm.

differentiate into pancreatic cells *in vivo* by implanting the cell aggregates on days 4–5 of Stage 4 into kidney subcapsule of immunocompromised mice. Thirty days after implantation, the aggregates had fused together to become single grafts (Fig. 6A). In contrast to the uniform distribution pattern of PDX1$^+$ cells inside aggregates before implantation (Fig. 4), PDX1$^+$ cells were well-aligned and formed tubular structures, which were observed throughout the entire grafts (Figs. 6B and C). There were INS$^+$ cells budding from tubular structures, as well as endocrine cell clusters (Fig. 6D), which were reminiscent of human embryonic pancreatic epithelia (Riedel et al., 2012). Most INS$^+$ cells were polyhormonal, co-expressing GCG, SST and GHR, without forming islet-like structures or co-expressing NKX6.1, and showed lower PDX1 expression levels compared with the surrounding tubular cells, thus indicating the generation of immature endocrine cells. Some PDX1$^+$ cells were not NKX6.1$^+$ but GATA4$^+$, implying the segregation of endocrine and exocrine lineages. These branched epithelial structures derived from implanted aggregates were observed in three independent experimental cohorts treated with KhES-3 hESCs (seven out of seven mice) and one independent cohort treated with 585A1 hiPSCs (one out of one mouse) (Fig. S6).

To confirm the differentiation potential of PDX1$^+$NKX6.1$^+$ cells into mature pancreatic β-cells, we examined plasma human C-peptide levels in host mice and the response to different blood glucose levels. To obtain a larger number of pancreatic β-cells *in vivo*, cellular aggregates were pre-treated with an ALK5 inhibitor before implantation, since this treatment was previously reported to promote the differentiation into β-cells (Rezania et al., 2012). We found

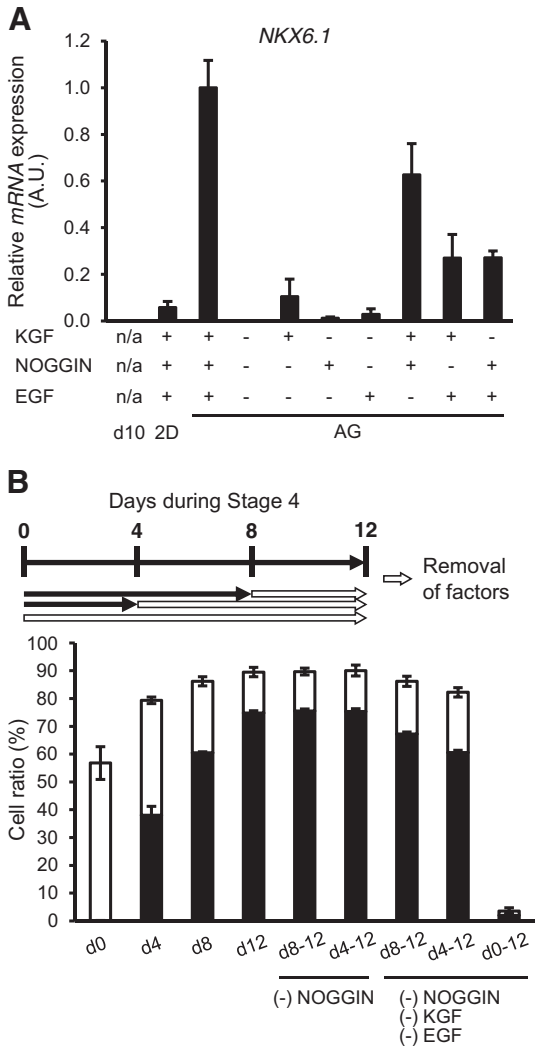

Figure 5 Both cell aggregation cultures and soluble factor treatment are required for the efficient induction of PDX1$^+$NKX6.1$^+$ cells. (A) *NKX6.1* expression was assessed by qRT-PCR in the cells treated with various combinations of soluble factors (100 ng/ml KGF, 100 ng/ml NOGGIN and 50 ng/ml EGF) for four days of Stage 4 aggregation culture. Cell aggregation alone did not induce the expression of *NKX6.1*. Treatment with all soluble factors with aggregation cultures most potently induced the expression of *NKX6.1*. (B) NOGGIN or all of the soluble factors (KGF, NOGGIN and EGF) was/were removed at the indicated periods during 12 days of aggregation culture at Stage 4. (Upper) A schematic diagram of the procedures used to assess the specific timing requirements for the soluble factors. (Lower) The quantification of the induction rate of PDX1$^+$NKX6.1$^+$ (black bars) and PDX1$^+$NKX6.1$^-$ (white bars) cells. The data are from three independent experiments presented as the mean ± S.E.M. n/a, not applicable.

that there was an about 10% increase in the NKX6.1$^+$ cell ratio by pre-treatment with the ALK5 inhibitor (data not shown). The human C-peptide levels in mouse plasma were gradually increased over time (Fig. 7A), and human C-peptide was detected in 11 out of 13 mice by 150 days after implantation (one mouse died before day 150). We found a similar tendency for a gradual increase in the human C-peptide levels in mice that underwent the implantation of cellular aggregates without the pre-treatment with an ALK5 inhibitor (data not shown). Moreover, we obtained grafts which were capable of responding to the changes in blood glucose levels by 150 days (Fig. 7B). There were also islet-like INS$^+$ cell clusters found inside the grafts, which did not co-express GCG on day 210 after implantation (Fig. 7C). These results suggest that the pancreatic cells generated with aggregation cultures have the developmental potential to differentiate into pancreatic epithelia and mature into β-cells *in vivo*.

Discussion

It has recently been demonstrated that hESCs/iPSCs can be differentiated into pancreatic lineages that show therapeutic potential for diabetes (Rezania et al., 2012, 2013; Bruin et al., 2013). Although the inducing factors have been intensively explored, the most suitable conditions to generate pancreatic cells have not yet been fully established. The obstacles preventing the establishment of such conditions include the different propensities for directed differentiation among hESC/iPSC lines (Osafune et al., 2008). We herein demonstrated that aggregation cultures efficiently induced the differentiation of pancreatic bud cells in multiple hESC/iPSC lines.

During embryonic development, the lineage commitment into the pancreas occurs at the step of pancreatic bud formation, in which Pdx1$^+$ cells form clusters and start expressing Ptf1a and Nkx6.1. A previous report utilized a rotational suspension-based differentiation method to generate PDX1$^+$NKX6.1$^+$ pancreatic bud progenitors from a hESC line, CyT49 (Schulz et al., 2012). Their use of cell aggregation cultures throughout the differentiation process from the undifferentiated state resulted in the efficient induction of PDX1$^+$NKX6.1$^+$ cells. Consistent with that study, we found that a higher cell density led to more efficient generation of PDX1$^+$NKX6.1$^+$ cells. Although the current model does not directly address the molecules responsible for these findings, the previous works and our current study allow us to hypothesize that a high cell density acts as a factor to activate the essential signals for the differentiation of posterior foregut cells into pancreatic bud.

Our findings suggest that the signals elicited by a high cell density or their surrogate stimuli are potent inducers of the directed differentiation of hESCs/iPSCs into pancreatic lineages. The efficient generation of PDX1$^+$NKX6.1$^+$ cells with adherent culture conditions in another report (Rezania et al., 2012) may have resulted from the acquisition of the signals due to the culture conditions or because the cell lines used intrinsically possessed the signals. Indeed, the increased cell number observed in Stage 1 resulted in a higher cell density at Stage 4, thus producing more efficient induction of NKX6.1$^+$ cells in the adherent cultures without re-seeding at Stage 4 (S4F; Supplementary Table 3). This result supports the idea that a high cell density is a key factor for pancreatic bud induction. We reason that unknown factors, including cell density factors, acting at specific times explain the variation in the differentiation efficiency noted in the different research groups. In the

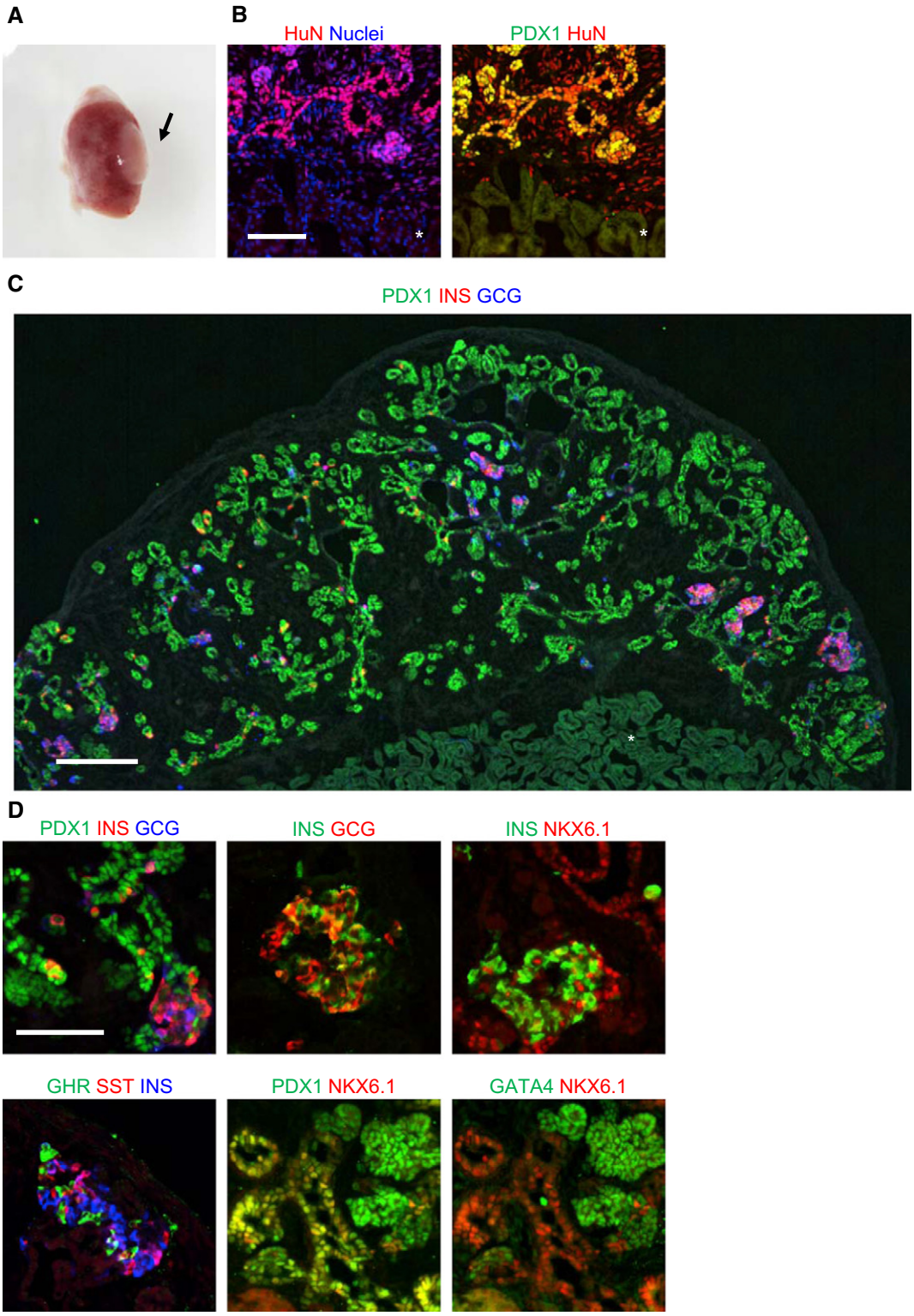

Figure 6 The PDX1^{+}NKX6.1^{+} cells generated with aggregation cultures differentiate into branched pancreatic epithelia *in vivo*. Cellular aggregates at Stage 4, days 4–5, were implanted into the kidney subcapsules of NOD–SCID mice. (A) An image of a host kidney harvested 30 days after implantation. The arrow indicates the location of the graft. (B–D) Cryosections of grafts were stained for the indicated markers. Representative images of human pancreatic cells are shown. Asterisks indicate the host mouse kidney in B and C. HuN, human nuclei. Scale bars, 100 μm in B and D and 300 μm in C.

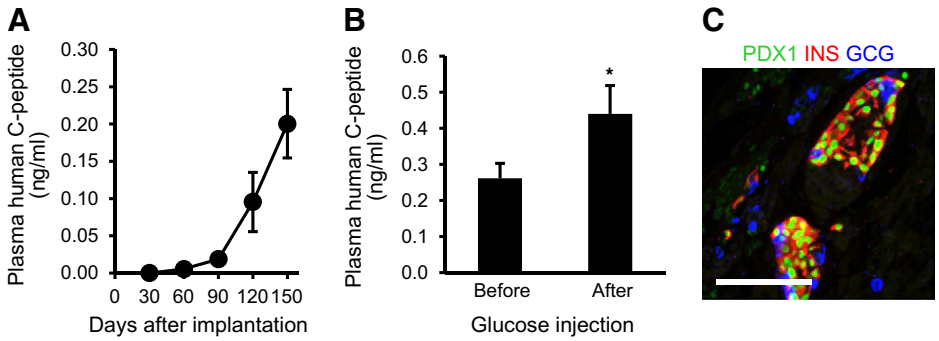

Figure 7 The PDX1$^+$NKX6.1$^+$ cells generated with aggregation cultures mature into functional β-cells *in vivo*. A total of six million cells at Stage 4, day 5, of aggregation cultures that had been pre-treated with an ALK5 inhibitor were implanted under the kidney subcapsule of NOD–SCID mice. (A) The average plasma human C-peptide levels in host mice were measured 30 min after glucose injection (3.0 g/ kg body weight, i.p.) at various time points after implantation, as indicated. (B) The average plasma human C-peptide levels after >5 h of fasting (before) and 30 min after glucose injection (after) in the host mice were examined on day 150 after implantation. (C) A representative image of hESC-derived islet-like endocrine clusters on day 210 after implantation. The data are presented as the mean ± S.E.M. of 13 mice from four independent cohorts of implantation experiments in A and four mice from two independent cohorts of implantation experiments in B. *$P < 0.05$. Scale bar, 100 μm.

present study, the induction rates of PDX1$^+$NKX6.1$^+$ cells were lower with some cell lines than with a hESC line, KhES-3. One plausible explanation is the low induction efficiency of cells in the steps before aggregation formation, such as definitive endoderm or posterior foregut cells. The optimization of culture conditions for these steps could make further contributions to resolving the problems of line-to-line variation of hESCs/iPSCs.

Although the detailed mechanisms underlying the increase in PDX1$^+$NKX6.1$^+$ cell induction in aggregation cultures remain unknown, this finding raises the possibility that pancreatic bud formation may be regulated by the molecules associated with contact-dependent cellular interactions, such as extracellular matrices and adhesion molecules, and other membrane-bound receptors (Brafman et al., 2013; Crisera et al., 2000; Ekblom et al., 1998). Possible mechanisms include the involvement of laminin–integrin signaling. During pancreatic development, epithelial cell delamination and migration into mesenchyme is the early event in the differentiation process into endocrine cells (Villasenor et al., 2012). However, we found that the expression levels of pan-laminin were similar between NKX6.1$^+$ cells and NKX6.1$^-$ cells in both aggregation and monolayer cultures (data not shown). Although we could not exclude the possibility that laminin isoforms are different between the cell populations, we assumed that typical laminin–integrin signals are not likely to be directly involved. In addition, based on the findings obtained with the other extracellular matrices (Fig. S1), at a minimum, laminin-111, vitronectin (main component of Synthemax), fibronectin and collagen I are not likely to be involved. Instead, other cell surface-derived signals, such as those associated with the apicobasal polarity (Villasenor et al., 2010; Kesavan et al., 2009) and planar cell polarity pathways (Cortijo et al., 2012), or unknown autocrine/paracrine molecules, may be involved. Further studies with comparative analyses of the gene expression profiles between 2D and aggregation cultures would be helpful to elucidate the factors responsible for the regulation of NKX6.1 induction in developing pancreatic buds.

It is possible that the signals elicited by a high cell density increased the ratio of PDX1$^+$NKX6.1$^+$ cells *via* the direct induction of differentiation into PDX1$^+$NKX6.1$^+$ cells, while the selective proliferation of progenitor cells and/or selective apoptosis of uncommitted cells are also possible mechanisms. The number of proliferating cells was low on days 1–2 in Stage 4, during which time the PDX1$^+$NKX6.1$^+$ cells emerged in the cell aggregation cultures (Figs. S5A and C). In addition, the total cell number in the aggregation cultures was not increased at Stage 4, days 1–2, suggesting the involvement of selective proliferation to be less likely (Fig. S3). On the other hand, the number of apoptotic cells was increased in the cellular aggregates, consistent with the idea that aggregation cultures selectively delete cells uncommitted to the PDX1$^+$NKX6.1$^+$ cell lineage (Figs. S5B and D). In fact, more apoptotic cells were found within the PDX1$^-$ cell population (Fig. S5D), which suggests that selective apoptosis is a possible mechanism. In the future, the identification of marker genes for pancreatic cells uncommitted to NKX6.1$^+$ cells and application of subsequent live cell imaging with the reporter cell line of the marker would help to clearly demonstrate the involvement of selective apoptosis in the increased PDX1$^+$NKX6.1$^+$ cell ratio observed in high-density cultures.

It was previously reported that the activation of BMP signaling facilitates the proliferation of NKX6.1$^+$ cells (Sui et al., 2013). In contrast, our data indicate that the inhibition by adding NOGGIN increased the *NKX6.1* expression (Fig. 5A). Consistent with our findings, other reports have demonstrated that NKX6.1$^+$ pancreatic progenitors were generated under continuous suppression of BMP signaling in hESC differentiation cultures (Rezania et al., 2012, 2013; Schulz et al., 2012; Bruin et al., 2013), and that the phosphorylation of smad1/5/8, downstream effectors of BMP signaling, was suppressed in Nkx6.1$^+$ cells from developing chick pancreatic buds (Ahnfelt-Ronne et al., 2010). In addition, the BMP inhibition by *in ovo* gene transfer of Noggin into the presumptive pancreatic region of chick embryos resulted in pancreatic bud formation without further branching and epithelialization (Ahnfelt-Ronne et al., 2010). We reasoned that BMP inhibition

is involved in the commitment to NKX6.1$^+$ cells, but that BMP signaling is necessary for the subsequent proliferation and differentiation. In agreement with this, we found that the induction rate of PDX1$^+$NKX6.1$^+$ cells was continuously increased with the removal of NOGGIN after day 4 of Stage 4 (Fig. 5B). Although BMP activation may expand NKX6.1$^+$ cells, we assume that the first four days of aggregation cultures are critical for the commitment of PDX1$^+$NKX6.1$^+$ cells, and that all three factors are beneficial for the PDX1$^+$NKX6.1$^+$ cell induction.

In summary, the cell density of PDX1$^+$ posterior foregut cells positively correlates with the induction of PDX1$^+$NKX6.1$^+$ pancreatic bud cells in hESC/iPSC differentiation cultures. Although the molecules that regulate the differentiation step remain unknown, the signals elicited by high cell density are crucial for the pancreatic bud induction, and synergistically work with soluble factors. To our knowledge, this is the first study clearly demonstrating that the signals derived from spatial and morphological contexts are associated with the differentiation of hESCs/iPSCs into pancreatic lineages. Further studies to elucidate the molecular nature of the signals based on our findings may contribute to the development of hESC/iPSC-based cell therapy for diabetes.

Supplementary data to this article can be found online at http://dx.doi.org/10.1016/j.scr.2015.01.007.

Acknowledgments

This work was supported in part by funding from the Takeda Science Foundation to T.T., the Suzuken Memorial Foundation to T.T. and the Life Science Foundation of Japan to K.O., by the Japan Society for the Promotion of Science (JSPS) through its 'Funding Programme for World-Leading Innovative R&D on Science and Technology (FIRST Programme)' to K.O. and Grant-in-Aid for Young Scientists (B) to T.T. and by the Japan Science and Technology Agency (JST) through its research grant "Core Center for iPS Cell Research and Projects for Technological Development, Research Center Network for Realization of Regenerative Medicine" to Y.K. and K.O. T.T. wrote the first draft of the manuscript. T.T., S.M., Y.K. and K.O. contributed to manuscript edits and revisions. T.T., S.M., Y.K., M.F., Y.H., Y.K. and K.O. designed, directed, and interpreted the experiments. T.T., S.M., H.T. and T.S. performed the experiments. K.O. supervised the study. The authors thank Kanae Mitsunaga for her technical assistance in the flow cytometry analysis and Yasuhiro Nakano for providing valuable advice on this research.

References

Ahnfelt-Ronne, J., Ravassard, P., Pardanaud-Glavieux, C., Scharfmann, R., Serup, P., 2010. Mesenchymal bone morphogenetic protein signaling is required for normal pancreas development. Diabetes 59, 1948–1956.

Ahnfelt-Ronne, J., Jorgensen, M.C., Klinck, R., Jensen, J.N., Fuchtbauer, E.M., Deering, T., MacDonald, R.J., Wright, C.V., Madsen, O.D., Serup, P., 2012. Ptf1a-mediated control of Dll1 reveals an alternative to the lateral inhibition mechanism. Development 139, 33–45.

Brafman, D.A., Phung, C., Kumar, N., Willert, K., 2013. Regulation of endodermal differentiation of human embryonic stem cells through integrin–ECM interactions. Cell Death Differ. 20, 369–381.

Bruin, J.E., Rezania, A., Xu, J., Narayan, K., Fox, J.K., O'Neil, J.J., Kieffer, T.J., 2013. Maturation and function of human embryonic stem cell-derived pancreatic progenitors in macroencapsulation devices following transplant into mice. Diabetologia 56, 1987–1998.

Cai, J., Yu, C., Liu, Y., Chen, S., Guo, Y., Yong, J., Lu, W., Ding, M., Deng, H., 2010. Generation of homogeneous PDX1(+) pancreatic progenitors from human ES cell-derived endoderm cells. J. Mol. Cell Biol. 2, 50–60.

Cortijo, C., Gouzi, M., Tissir, F., Grapin-Botton, A., 2012. Planar cell polarity controls pancreatic beta cell differentiation and glucose homeostasis. Cell Rep. 2, 1593–1606.

Crisera, C.A., Kadison, A.S., Breslow, G.D., Maldonado, T.S., Longaker, M.T., Gittes, G.K., 2000. Expression and role of laminin-1 in mouse pancreatic organogenesis. Diabetes 49, 936–944.

D'Amour, K.A., Bang, A.G., Eliazer, S., Kelly, O.G., Agulnick, A.D., Smart, N.G., Moorman, M.A., Kroon, E., Carpenter, M.K., Baetge, E.E., 2006. Production of pancreatic hormone-expressing endocrine cells from human embryonic stem cells. Nat. Biotechnol. 24, 1392–1401.

Dominguez-Bendala, J., Inverardi, L., Ricordi, C., 2011. Stem cell-derived islet cells for transplantation. Curr. Opin. Organ Transplant. 16, 76–82.

Donath, M.Y., Halban, P.A., 2004. Decreased beta-cell mass in diabetes: significance, mechanisms and therapeutic implications. Diabetologia 47, 581–589.

Ekblom, M., Falk, M., Salmivirta, K., Durbeej, M., Ekblom, P., 1998. Laminin isoforms and epithelial development. Ann. N. Y. Acad. Sci. 857, 194–211.

Fukuda, A., Kawaguchi, Y., Furuyama, K., Kodama, S., Kuhara, T., Horiguchi, M., Koizumi, M., Fujimoto, K., Doi, R., Wright, C.V., Chiba, T., 2006. Loss of the major duodenal papilla results in brown pigment biliary stone formation in pdx1 null mice. Gastroenterology 130, 855–867.

Hald, J., Sprinkel, A.E., Ray, M., Serup, P., Wright, C., Madsen, O.D., 2008. Generation and characterization of Ptf1a antiserum and localization of Ptf1a in relation to Nkx6.1 and Pdx1 during the earliest stages of mouse pancreas development. J. Histochem. Cytochem. 56, 587–595.

Jennings, R.E., Berry, A.A., Kirkwood-Wilson, R., Roberts, N.A., Hearn, T., Salisbury, R.J., Blaylock, J., Piper Hanley, K., Hanley, N.A., 2013. Development of the human pancreas from foregut to endocrine commitment. Diabetes 62, 3514–3522.

Jensen, J., 2004. Gene regulatory factors in pancreatic development. Dev. Dyn. 229, 176–200.

Jiang, W., Shi, Y., Zhao, D., Chen, S., Yong, J., Zhang, J., Qing, T., Sun, X., Zhang, P., Ding, M., Li, D., Deng, H., 2007a. In vitro derivation of functional insulin-producing cells from human embryonic stem cells. Cell Res. 17, 333–344.

Jiang, J., Au, M., Lu, K., Eshpeter, A., Korbutt, G., Fisk, G., Majumdar, A.S., 2007b. Generation of insulin-producing islet-like clusters from human embryonic stem cells. Stem Cells 25, 1940–1953.

Jorgensen, M.C., Ahnfelt-Ronne, J., Hald, J., Madsen, O.D., Serup, P., Hecksher-Sorensen, J., 2007. An illustrated review of early pancreas development in the mouse. Endocr. Rev. 28, 685–705.

Kajiwara, M., Aoi, T., Okita, K., Takahashi, R., Inoue, H., Takayama, N., Endo, H., Eto, K., Toguchida, J., Uemoto, S., Yamanaka, S., 2012. Donor-dependent variations in hepatic differentiation from human-induced pluripotent stem cells. Proc. Natl. Acad. Sci. U. S. A. 109, 12538–12543.

Kawaguchi, Y., Cooper, B., Gannon, M., Ray, M., MacDonald, R.J., Wright, C.V., 2002. The role of the transcriptional regulator Ptf1a in converting intestinal to pancreatic progenitors. Nat. Genet. 32, 128–134.

Kelly, O.G., Chan, M.Y., Martinson, L.A., Kadoya, K., Ostertag, T.M., Ross, K.G., Richardson, M., Carpenter, M.K., D'Amour, K.A., Kroon, E., Moorman, M., Baetge, E.E., Bang, A.G., 2011. Cell-surface markers for the isolation of pancreatic cell types derived from human embryonic stem cells. Nat. Biotechnol. 29, 750–756.

Kesavan, G., Sand, F.W., Greiner, T.U., Johansson, J.K., Kobberup, S., Wu, X., Brakebusch, C., Semb, H., 2009. Cdc42-mediated tubulogenesis controls cell specification. Cell 139, 791–801.

Kroon, E., Martinson, L.A., Kadoya, K., Bang, A.G., Kelly, O.G., Eliazer, S., Young, H., Richardson, M., Smart, N.G., Cunningham, J., Agulnick, A.D., D'Amour, K.A., Carpenter, M.K., Baetge, E.E., 2008. Pancreatic endoderm derived from human embryonic stem cells generates glucose-responsive insulin-secreting cells in vivo. Nat. Biotechnol. 26, 443–452.

Kunisada, Y., Tsubooka-Yamazoe, N., Shoji, M., Hosoya, M., 2012. Small molecules induce efficient differentiation into insulin-producing cells from human induced pluripotent stem cells. Stem Cell Res. 8, 274–284.

Mae, S., Shono, A., Shiota, F., Yasuno, T., Kajiwara, M., Gotoda-Nishimura, N., Arai, S., Sato-Otubo, A., Toyoda, T., Takahashi, K., Nakayama, N., Cowan, C.A., Aoi, T., Ogawa, S., McMahon, A.P., Yamanaka, S., Osafune, K., 2013. Monitoring and robust induction of nephrogenic intermediate mesoderm from human pluripotent stem cells. Nat. Commun. 4, 1367.

Mathis, D., Vence, L., Benoist, C., 2001. Beta-cell death during progression to diabetes. Nature 414, 792–798.

Matsumoto, S., 2011. Clinical allogeneic and autologous islet cell transplantation: update. Diabetes Metab. J. 35, 199–206.

McCall, M.D., Toso, C., Baetge, E.E., Shapiro, A.M., 2010. Are stem cells a cure for diabetes? Clin. Sci. (Lond.) 118, 87–97.

Mfopou, J.K., Chen, B., Mateizel, I., Sermon, K., Bouwens, L., 2010. Noggin, retinoids, and fibroblast growth factor regulate hepatic or pancreatic fate of human embryonic stem cells. Gastroenterology 138, 2233–2245 (2245 e2231–2214).

Nostro, M.C., Sarangi, F., Ogawa, S., Holtzinger, A., Corneo, B., Li, X., Micallef, S.J., Park, I.H., Basford, C., Wheeler, M.B., Daley, G.Q., Elefanty, A.G., Stanley, E.G., Keller, G., 2011. Stage-specific signaling through TGFbeta family members and WNT regulates patterning and pancreatic specification of human pluripotent stem cells. Development 138, 861–871.

Okita, K., Matsumura, Y., Sato, Y., Okada, A., Morizane, A., Okamoto, S., Hong, H., Nakagawa, M., Tanabe, K., Tezuka, K., Shibata, T., Kunisada, T., Takahashi, M., Takahashi, J., Saji, H., Yamanaka, S., 2011. A more efficient method to generate integration-free human iPS cells. Nat. Methods 8, 409–412.

Osafune, K., Caron, L., Borowiak, M., Martinez, R.J., Fitz-Gerald, C.S., Sato, Y., Cowan, C.A., Chien, K.R., Melton, D.A., 2008. Marked differences in differentiation propensity among human embryonic stem cell lines. Nat. Biotechnol. 26, 313–315.

Oster, A., Jensen, J., Serup, P., Galante, P., Madsen, O.D., Larsson, L.I., 1998. Rat endocrine pancreatic development in relation to two homeobox gene products (Pdx-1 and Nkx 6.1). J. Histochem. Cytochem. 46, 707–715.

Pan, F.C., Bankaitis, E.D., Boyer, D., Xu, X., Van de Casteele, M., Magnuson, M.A., Heimberg, H., Wright, C.V., 2013. Spatiotemporal patterns of multipotentiality in Ptf1a-expressing cells during pancreas organogenesis and injury-induced facultative restoration. Development 140, 751–764.

Rezania, A., Riedel, M.J., Wideman, R.D., Karanu, F., Ao, Z., Warnock, G.L., Kieffer, T.J., 2011. Production of functional glucagon-secreting alpha-cells from human embryonic stem cells. Diabetes 60, 239–247.

Rezania, A., Bruin, J.E., Riedel, M.J., Mojibian, M., Asadi, A., Xu, J., Gauvin, R., Narayan, K., Karanu, F., O'Neil, J.J., Ao, Z., Warnock, G.L., Kieffer, T.J., 2012. Maturation of human embryonic stem cell-derived pancreatic progenitors into functional islets capable of treating pre-existing diabetes in mice. Diabetes 61, 2016–2029.

Rezania, A., Bruin, J.E., Xu, J., Narayan, K., Fox, J.K., O'Neil, J.J., Kieffer, T.J., 2013. Enrichment of human embryonic stem cell-derived NKX6.1-expressing pancreatic progenitor cells accelerates the maturation of insulin-secreting cells in vivo. Stem Cells 31, 2432–2442.

Riedel, M.J., Asadi, A., Wang, R., Ao, Z., Warnock, G.L., Kieffer, T.J., 2012. Immunohistochemical characterisation of cells co-producing insulin and glucagon in the developing human pancreas. Diabetologia 55, 372–381.

Schulz, T.C., Young, H.Y., Agulnick, A.D., Babin, M.J., Baetge, E.E., Bang, A.G., Bhoumik, A., Cepa, I., Cesario, R.M., Haakmeester, C., Kadoya, K., Kelly, J.R., Kerr, J., Martinson, L.A., McLean, A.B., Moorman, M.A., Payne, J.K., Richardson, M., Ross, K.G., Sherrer, E.S., Song, X., Wilson, A.Z., Brandon, E.P., Green, C.E., Kroon, E.J., Kelly, O.G., D'Amour, K.A., Robins, A.J., 2012. A scalable system for production of functional pancreatic progenitors from human embryonic stem cells. PLoS One 7, e37004.

Serup, P., Petersen, H.V., Pedersen, E.E., Edlund, H., Leonard, J., Petersen, J.S., Larsson, L.I., Madsen, O.D., 1995. The homeodomain protein IPF-1/STF-1 is expressed in a subset of islet cells and promotes rat insulin 1 gene expression dependent on an intact E1 helix–loop–helix factor binding site. Biochem. J. 310 (Pt 3), 997–1003.

Shim, J.H., Kim, S.E., Woo, D.H., Kim, S.K., Oh, C.H., McKay, R., Kim, J.H., 2007. Directed differentiation of human embryonic stem cells towards a pancreatic cell fate. Diabetologia 50, 1228–1238.

Suemori, H., Yasuchika, K., Hasegawa, K., Fujioka, T., Tsuneyoshi, N., Nakatsuji, N., 2006. Efficient establishment of human embryonic stem cell lines and long-term maintenance with stable karyotype by enzymatic bulk passage. Biochem. Biophys. Res. Commun. 345, 926–932.

Sui, L., Geens, M., Sermon, K., Bouwens, L., Mfopou, J.K., 2013. Role of BMP signaling in pancreatic progenitor differentiation from human embryonic stem cells. Stem Cell Rev. 9, 569–577.

Villasenor, A., Chong, D.C., Henkemeyer, M., Cleaver, O., 2010. Epithelial dynamics of pancreatic branching morphogenesis. Development 137, 4295–4305.

Villasenor, A., Marty-Santos, L., Dravis, C., Fletcher, P., Henkemeyer, M., Cleaver, O., 2012. EphB3 marks delaminating endocrine progenitor cells in the developing pancreas. Dev. Dyn. 241, 1008–1019.

Xu, X., Browning, V.L., Odorico, J.S., 2011. Activin, BMP and FGF pathways cooperate to promote endoderm and pancreatic lineage cell differentiation from human embryonic stem cells. Mech. Dev. 128, 412–427.

Zhang, D., Jiang, W., Liu, M., Sui, X., Yin, X., Chen, S., Shi, Y., Deng, H., 2009. Highly efficient differentiation of human ES cells and iPS cells into mature pancreatic insulin-producing cells. Cell Res. 19, 429–438.